GPS reference station siting tool

Christophe Macabiau, Benoit Roturier, Eric Chatre, Alain Renard

GPS Reference Station Siting Tool

Christophe MACABIAU, Benoît ROTURIER, *CNS Research Laboratory of the ENAC*
Eric CHATRE**,** *STNA*
ALAIN RENARD**,** *SEXTANT*

BIOGRAPHY

Christophe Macabiau is in charge of the signal processing unit of the CNS Research Laboratory (URE-CNS) at the Ecole Nationale de l'Aviation Civile (ENAC) in Toulouse, France. After working in 1993 for the MLS Project Office in Ottawa, Canada, he received his Ph.D. from the Laboratoire de Traitement du Signal et des Télécommunications of the ENAC in 1997. He is currently working on the application of code and phase LADGPS positioning techniques to aeronautics.

Benoît Roturier graduated as an electronics engineer in 1985 from the Ecole Nationale de l'Aviation Civile (ENAC), Toulouse, France. After working for 18 months at Tahiti Faaa airport, French Polynesia, he led the Instrument Landing Team at the Service Technique de la Navigation Aérienne (STNA) in Paris from 1987 to 1989. Since 1990, he has been teaching and doing research at the ENAC, where he is currently in charge of the CNS Research Laboratory. He obtained his Ph.D. in 1995 from the Institut National Polytechnique de Toulouse (INPT). His current research area is propagation modeling for aeronautical telecommunication systems.

Eric Chatre graduated as an electronics engineer in 1992 from the ENAC (Ecole Nationale de l'Aviation Civile), Toulouse, France. Since 1994, he has been working with the Service Technique de la Navigation Aérienne (STNA) in Toulouse. He is involved in GNSS standardization activities in ICAO GNSSP and EUROCAE, RTCA forums.

Alain Renard is a GPS expert in the Advanced Studies division of the Navigation Department of SEXTANT. After graduating in 1972 as an engineer from the Ecole Nationale Supérieure d'Electronique et de Radioélectricité of Grenoble, he worked on radionavigation systems for commercial aircraft from 1973 to 1978. Then, he developed radionavigation systems based on OMEGA until 1988. Since 1988, he has been designing GPS and GLONASS navigation systems.

ABSTRACT

The CNS Research Laboratory (URE-CNS) of the ENAC, in collaboration with the STNA and SEXTANT AVIONIQUE, is developing a tool for providing DGPS reference stations siting guidelines for the French Civil Aviation Authority. This tool is based on computed error predictions using mathematical models, and on signal disturbance measurements made at pre-selected locations. The aim of the proposed paper is to present the complete siting tool which was developed along with some examples of its use showing the extent of the validity of its predictions.

I. INTRODUCTION

The siting of a GPS reference station on an airport is achieved by minimizing the influence of the environment on the pseudorange measurements, while complying with the practical operational installation constraints. The CNS Research Laboratory (URE-CNS) of the ENAC, in collaboration with the STNA and SEXTANT AVIONIQUE, has started a study that aims at providing siting guidelines for the French Civil Aviation Authority [Macabiau et al., 1998].

As a result, a tool is developed, based on computed error predictions using mathematical models, and on signal disturbance measurements made at pre-selected locations. The first part of this tool is an end-to-end GPS simulator that is used to establish the main basic rules for the choice of the best configuration and location of the station on an airport with regards to multipath effects by providing analysis of the measurement errors induced by simple obstacles [Macabiau et al., 1999]. The second part of this tool is software designed to extract the measurement errors from the observations made by a GPS receiver connected to an antenna placed at the surveyed location.

The aim of this paper is to present the complete siting tool which was developed along with some examples of its application.

II. END-TO-END GPS SIMULATOR

The end-to-end GPS simulator is software that simulates the effect of multipath on a GPS receiver. The input data is the position of the satellites at various epochs. The output data are the GPS observation errors, such as the pseudorange measurement errors. The simulation is done using three cascaded processing modules written in MATLAB, that exchange data as illustrated in figure 1.

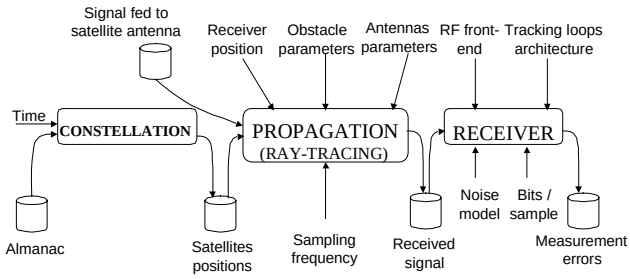

Figure 1: *Architecture of the end-to-end GPS simulator.*

- The constellation module determines the positions of the GPS satellites in the WGS-84 reference frame using the input almanac file and the specified transmission time. The period used to sample the position of the satellites is equal to the sampling period of the transfer function of the propagation channel.
- The propagation module combines ray-tracing software based on the Uniform Theory of Diffraction adapted to GPS signals, and a signal generator that computes the baseband equivalent spectrum of the signal received from a particular satellite by the receiving antenna.
- The received signal is computed by filtering the signal fed to the transmitting antenna of the satellite by the calculated transfer function of the channel. The receiver module contains a model of a GPS receiver that simulates the operations performed by a receiver, in order to determine the measurement errors induced by multipath. The program computes the code and phase tracking errors by searching for the code and phase delay estimates that cancel the PLL and DLL control signals.

Figure 2 shows an illustration of the contents of the propagation channel as it was defined for this study. The propagation channel contains any element from the satellite antenna connector to the receiving antenna connector.

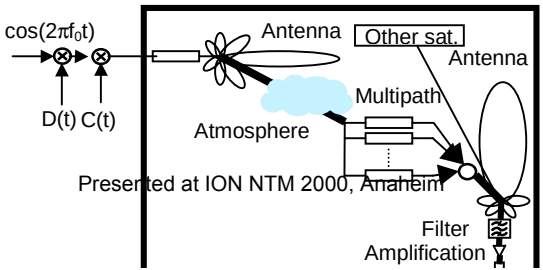

Figure 2: *Description of the propagation channel as it is used for this study.*

Specific models of the propagation channel and of the receiver processing operations were developed and inserted in the simulator. The propagation channel of a particular satellite signal is modeled as a linear time variant filter *h*, as presented in equation (1):

$$r(t) = \int_{-\infty}^{+\infty} s(t-\tau)h(\tau;t)d\tau \qquad (1)$$

where

- *s* is the signal fed to the transmitting antenna of the satellite. In our case, *s* is the power wave sent to the antenna.
- *r* is the signal delivered by the receiving antenna. In our case, *r* is the power wave sent to the receiver front-end.
- τ is the argument of the weighting function *h* used to compute the filter output.
- *t* is the time at which the transfer function of the channel is applied.

For a better understanding of this time varying channel model, the time variable *t* can be related to the position of the transmitting satellite at that particular time. Therefore, $h(\tau;t)$ can be viewed as the impulse response of the propagation channel related to a particular position of the satellite with respect to the receiver and the surrounding obstacles.

In the case where the multipath affecting the signal is countable, we can propose the following simple mathematical model of the physical channel:

$$h(\tau;t) = \sum_{n=0}^{N(t)} h_n(\tau;t) \qquad (2)$$

where

- h_n is the impulse response of the channel associated to each path *n*. In general, h_n relates to a dispersive medium.
- $N(t)$ is the number of distorted replicas of the transmitted signal delivered by the receiver antenna. This number varies with time.

The Fourier transform of *h* with respect to τ with *t* fixed is the transfer function of the channel at time *t*. If the perturbations associated to each replica *n* can be restricted

to a delay and an attenuation both variable with time and frequency, then its general expression is:

$$H(f;t) = \sum_{n=0}^{N(t)} \alpha_n(f;t) e^{-i\varphi_n(f;t)} \qquad (3)$$

where

- $\alpha_n(f;t)$ is the total attenuation. $\alpha_n(f;t)$ is a positive number, representative of the magnitude of the transfer function of each ray. This term depends on the free space loss, on the reflection and diffraction coefficients, on the antenna gains and polarization losses.
- $\varphi_n(f;t)$ is the total phase shift. The propagation of the waves along the ray creates a rotation depending on the propagation delay. Moreover, when hitting each obstacle, the phase of the signal is affected by a sudden jump. In addition, the position of the antennas phase center may vary with frequency, as well as with the directions of departure and arrival. Finally, the polarization mismatch between the incoming wave and the receiving antenna creates a phase jump of the received signal.

These parameters of the propagation channel are determined by the propagation module, which is based on a ray-tracing software.

In order to reduce the computation time, the propagation channel is sampled with a time interval larger than the internal sampling period of the receiver. As explained in [Macabiau et al., 1998], the transfer function is determined with a period lower than the time of coherence of the channel, which is of the order of a few seconds. At each one of these sampling epochs, the characteristics of the channel are assumed to be constant over a short interval, and a short slice of the received signal will be generated by filtering the signal fed to the satellite antenna through the predicted propagation channel transfer function.

As a consequence, at each one of the sampling step, that transfer function must be determined around L1 on a bandwidth that has to be at least as large as the RF front-end pre-correlation filter bandwidth. The transfer function is sampled around L1 with a frequency step Δf. The Shannon theorem states that a signal must be sampled at a rate larger than twice the bandwidth of its Fourier transform. As recalled in [Macabiau et al., 1998], the bandwidth of the Fourier transform of the transfer function of the channel is called the multipath delay spread, which is the inverse of the coherence bandwidth of the channel. Therefore, the transfer function of the channel is sampled with a frequency step lower or equal to half the coherence bandwidth of the channel.

The signal delivered by the receiving antenna to the receiver front-end is computed as the result of the filtering of the input signal by the propagation channel transfer function. The transfer function determined by the propagation module with a frequency step Δf is further interpolated so that the filtering operation is performed in the frequency domain by multiplying the input signal spectrum by the interpolated transfer function.

The transfer function *h* is determined by the ray-tracing software. The kernel of this software, called MUSICA (MUltipath SImulation for Civil Aviation) was developed by the ENAC for classical navaids [Roturier B., 1996]. This part of the software is based on the Uniform Theory of Diffraction (UTD).

This computed signal is then sent to the receiver simulation module. This receiver simulation module is composed of an RF front-end simulator and of the tracking loop simulator.

The operations performed within the RF front end are modeled as ideal amplification, frequency transposition, sampling and quantization, as depicted in figure 3.

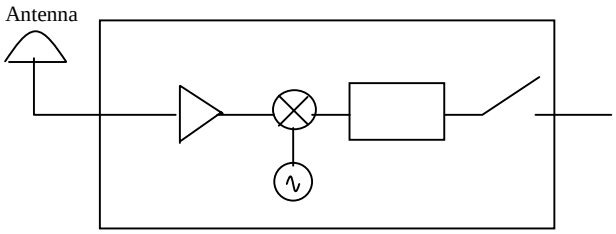

Figure 3: *Model of the RF front-end used in the simulator.*

The signal is then sent to the tracking loops. Figure 4 is an illustration of the architecture of the simulated tracking loops.

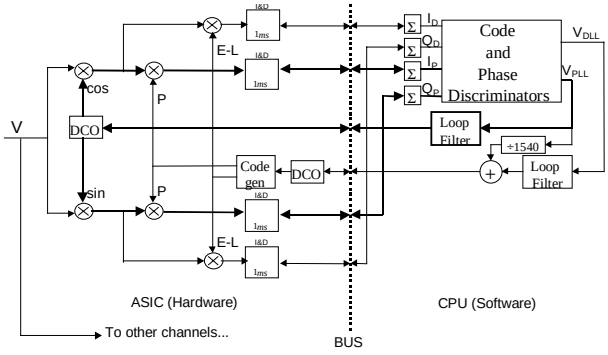

Figure 4: *Architecture of a digital GPS receiver.*

III. MEASUREMENT TOOL

The measuring tool uses the raw data collected by a dual frequency GPS receiver to isolate the measurement errors made by the code tracking loop caused by multipath. The technique consists in forming a multipath observable by summing the code and phase measurements. This multipath observable contains the

code and phase tracking errors due to multipath and noise, and is not affected by the satellite-user range variation, nor by the common errors such as tropospheric delay and satellite clock offset, including SA [Braasch, 1996].

The ionospheric divergence contained in the multipath observable is removed by subtracting an estimate of the ionospheric delay formed using the L1 and L2 carrier phase pseudorange measurements, as suggested in [Braasch, 1994]. As the carrier phase observations are less susceptible to multipath, this estimate of the ionospheric delay is less affected by multipath than the classical estimate computed using the code pseudorange measurements. However, this estimate is biased because the carrier phase measurements have an intrinsic ambiguity. This has no importance because the multipath observable is biased by the L1 carrier phase measurement ambiguity anyway.

Once the ionospheric divergence is removed, only remains the code and phase tracking errors due to noise and multipath plus the bias contained in the ionospheric delay estimate and the L1 carrier phase measurement. Assuming the phase tracking errors are negligible compared to their code counterparts, the remaining quantities are the code tracking tracking error due to noise and multipath plus a bias. Note that the bias is removed by subtracting the mean value of this quantity over a given interval. This operation also removes the average value of the multipath error, only leaving the non-zero frequency components. Moreover, as carrier phase measurements are intensively used in this technique, the resulting quantity may be affected by cycle slips, especially at low elevation angles when multipath is severe and the carrier to noise density ratio is low.

The code measurements used by the measuring tool are smoothed using the L1 carrier phase measurements with a 2s smoothing filter. This reduces the noise level, while keeping most of the multipath frequency components, as the antenna is fixed on the ground.

Therefore, the code tracking errors can be isolated from this quantity provided that the PLL and the DLL maintain continuous tracking. Besides any other obvious condition, this is true if the multipath is not too severe to cause a PLL or DLL loss of lock.

IV. COMPLETE SITING TOOL

The complete siting tool is composed of the simulation and the measurement tool. Both tools are complementary.

First of all, a model of the real situation is developed. The environment, the antenna and the receiver are modeled and these models are inserted in the simulation tool. Then, simulations are run to determine a set of predicted errors in the modeled situations. This enables us to establish some preliminary siting rules, and is used to select some of the envisaged situations as potential candidates for an operational siting. For each of the selected situations, the measuring tool is used, and the output observed errros are used to determine the final siting location and configuration.

V. EXAMPLES

The simulator has undergone a theoretical and a practical validation to check the validity of its predictions.

The theoretical validation has consisted in comparing the predicted code and phase tracking errors in simple artificial well-known situations, involving only one reflector (ground or building wall), with the theoretical tracking errors. This first validation allowed to correct a few bugs in the software, and the final results showed no failure of the simulator.

The practical validation consists in comparing the predicted code tracking errors in simple situations with the observed real tracking errors in the same situations. The parameters provided to the simulator where chosen to reflect the real situation as closely as we could. The position and height of the antenna on the ground and its distance with respect to the obstacles was measured and inserted in the propagation module. The digitized RHC and LHC patterns of the antennas used for the measurements were fed to the propagation module. The receiver parameters, such as the RF front-end filter bandwidth and the global tracking loop parameters were inserted in the receiver simulation module.

Several sets of measurements were collected in various situations involving different types of obstacles. We present here some results of comparison of measurements and simulation when the main obstacles are the ground and one building.

The first set of measurements presented in this paper was collected on the site of the Toulouse-Blagnac airport DGPS reference station, in a direction where the main reflector is assumed to be only the ground. Figures 5, 6, 7 and 8 show the observed and the simulated values obtained using a choke ring antenna placed 6.6 meters above the ground.

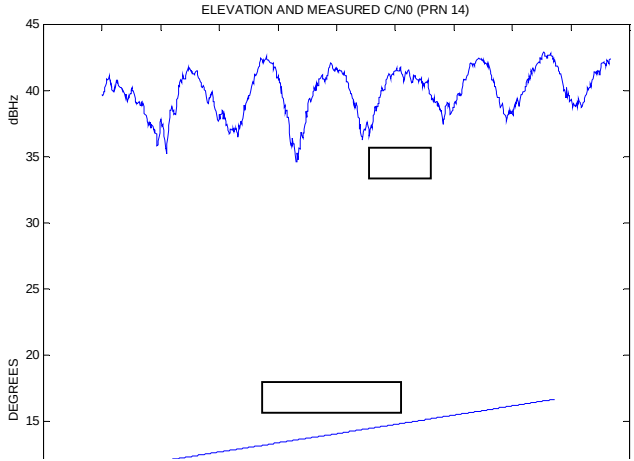

Figure 5: *Measured C/N0 for a choke ring antenna 6.6 m above the ground (PRN 14).*

Figure 5 shows the elevation and the measured C/N_0 for PRN 14. As we can see for this rising satellite, the long term evolution of the measured C/N_0 shows that the incoming signal is affected by one reflected signal. But we can also see that faster variations exist, indicating the presence of other diffracted rays.

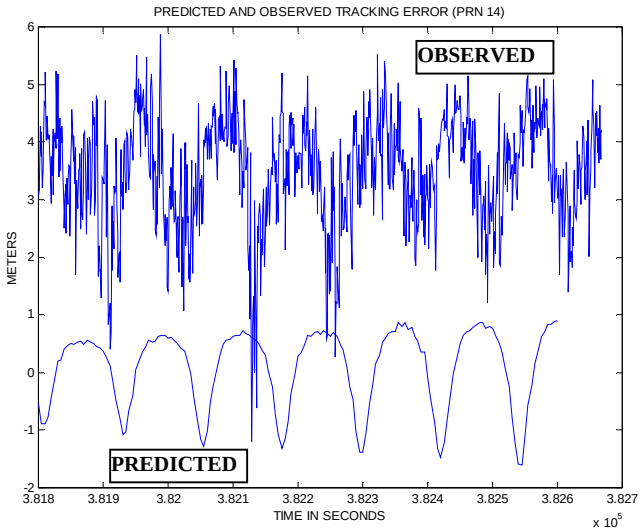

Figure 6: *Comparison of predicted and observed code tracking error for a choke ring antenna 6.6 m above the ground (PRN 14).*

The upper part of figure 6 shows the extracted code measurement error due to noise and multipath obtained using the technique presented in section II. The error has a high frequency component due to the noise that has a meter level amplitude on this plot. The error has also a low frequency component that can be attributed to multipath. The amplitude of this component is approximately 2 meters, and its period is about 110 s. This period is characteristic of the time required for the ray reflected by the Earth's surface to rotate by one complete L1 wavelength with respect to the direct signal at the antenna phase center located approximately at 6.6 m above the ground.

The lower part of figure 6 shows the predicted tracking error obtained using the simulator. The only obstacle inserted in the simulator is the Earth's surface modeled as a metallic plate. As we can see, the period and the amplitude of the predicted error are compatible with the observed values. The only difference is a phase shift that can be explained by the difficulty to set the dielectric parameters of the soil at this time, and the uncertainty in the height of the antenna above the reflecting ground plane. But this phase shift is not important in this application as the objective is to predict as accurately as possible the shape and the amplitude of the tracking error due to multipath.

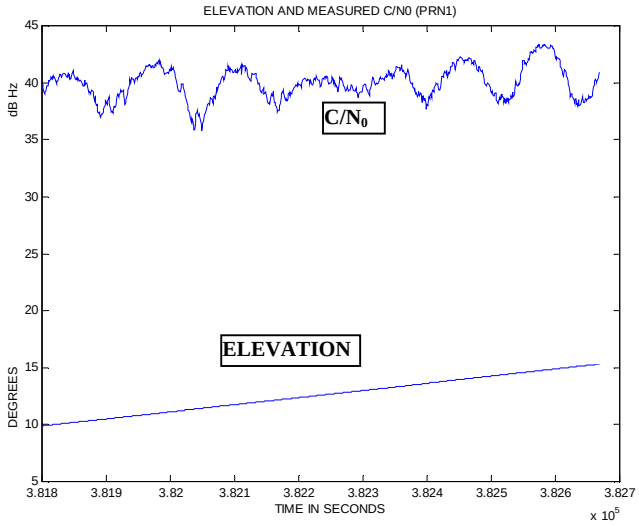

Figure 7: *Measured C/N0 for a choke ring antenna 6.6 m above the ground (PRN 1).*

Figure 7 shows the elevation and the measured C/N_0 for PRN 1. Comparing this figure with figure 5 shows that the signal is mainly affected by one reflected ray, but another phenomenon disturbs the signal in the middle of the time interval This could be due to another reflected ray coming from another obstacle, or to a change in the ray reflected by the ground at this point.

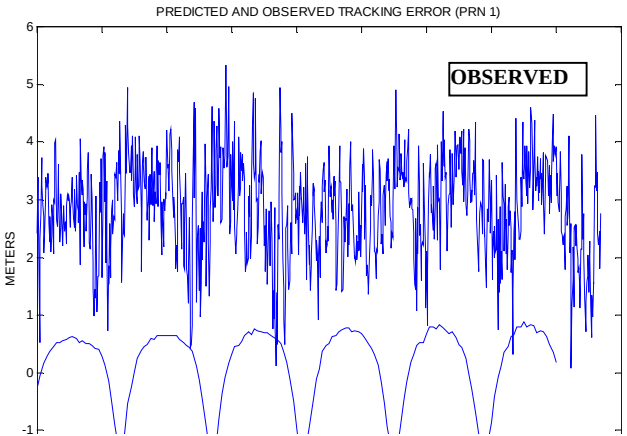

Figure 8: *Comparison of predicted and observed code tracking error for a choke ring antenna 6.6 m above the ground (PRN 1).*

The upper curve of figure 8 shows the observed tracking error extracted using the technique presented in section II. As we can see, this curve is highly similar to the curve presented in figure 6, with the exception of the middle interval of the plot.

The lower part of figure 8 shows the predicted code tracking error obtained using the simulator. As we can see, the predicted error corresponds to the long term variation of the curve with the exception that the flatness of the observed error in the middle of the time interval is not reproduced. This deviation between the observed and predicted errors is due to the fact that all the obstacles were not accurately modeled in the simulator. In particular, the DGPS reference station shelter was not modeled in this particular trial.

The second set of measurements presented here was collected on the ENAC campus, and involves one building and the ground. The antenna is a classical patch GPS antenna placed 2.15 m above the ground and 5.5 m away from a building wall that is 5.65 m high. Figures 10 and 11 show the collected and the simulated values obtained in this situation, for a satellite with an elevation decreasing from 13 degrees to below the mask angle.

Figure 9 shows all the second order interaction rays that the simulator could determine for that situation. We see that the direct ray is combined with several rays. Among those, are a ray reflected by the ground, a ray reflected by the building wall, a ray reflected by the ground and by the wall, plus diffracted rays.

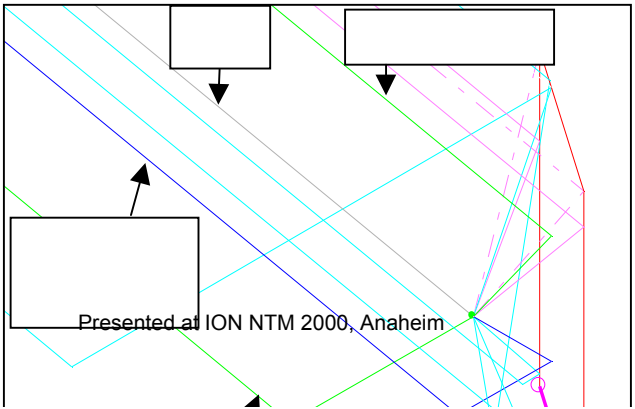

Figure 9: *Result of the ray tracing operation performed by the simulator.*

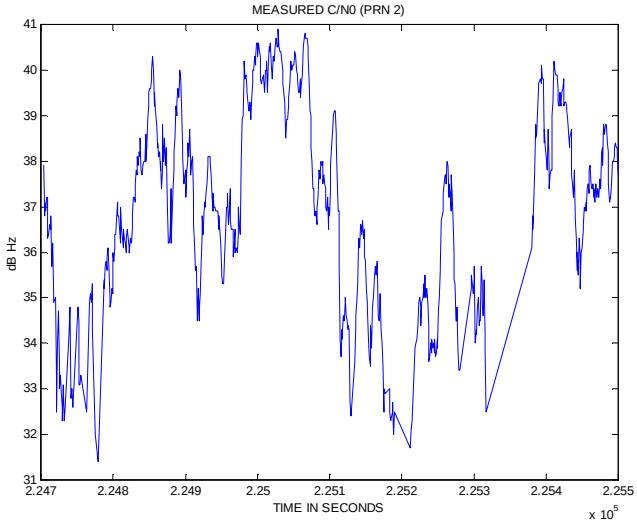

Figure 10: *Measured C/N0 for a patch antenna 2.15 m above the ground and close to a building.*

Figure 10 shows the elevation and the measured C/N_0 for PRN 2. As we can see, the measured C/N_0 shows that the signal is disturbed in a different way than in the previous cases, as we can see by comparing figures 5 and 10. The C/N_0 even goes down under the tracking threshold, causing the loops to lose lock several times during this interval. Clearly, there are more than one reflected ray entering the tracking loops.

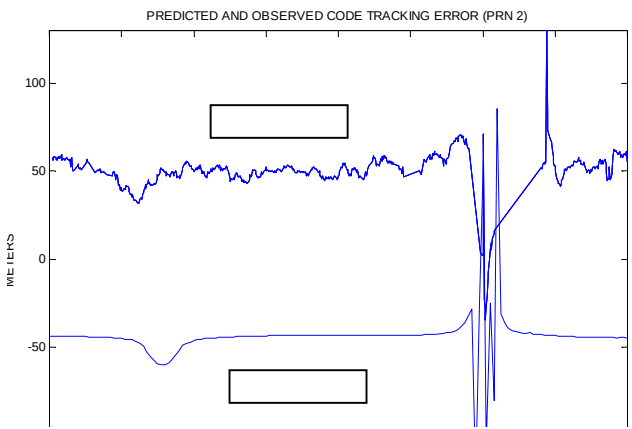

Figure 11: *Comparison of predicted and observed code tracking error for a patch antenna 2.15 m above the ground and close to a building.*

The upper part of figure 11 shows the extracted code tracking error using the technique presented in section II. As we can see, the error is much larger than in the previous case, and the final part shows that the loops have lost track of the signal for a moment. As in the previous case, the curve has a high frequency component due to the noise, and a low frequency component that has large variations which is attributed to multipath.

The lower part of figure 11 shows the code tracking error that is predicted using the simulator. We can see that the predicted tracking error has the same large scale variations as the observed error, with a slight delay in time. In particular, the predicted error drops down by about 10 meters in the beginning, and it is erratic at the end, just like the observed error. This kind of result could only be achieved by taking into account the two major obstacles interacting with the signal, namely the Earth's surface and the building wall. However, smaller variations of the low frequency component visible on the upper plot of figure 11 could not be reproduced, and may be attributed to other obstacles that were not modeled.

II. CONCLUSION

The siting tool presented in this paper is composed of a simulator and a measuring tool.

The simulator has undergone a theoretical and practical validation process which is about to be finished. The first results of this validation process showed that the simulator could predict the code tracking error with a satisfying accuracy when only simple obstacles are involved, such as the ground and buildings. These results also confirmed that the simulator can not precisely predict the tracking errors when the environment can not be modeled with a sufficient accuracy.

ACKNOWLEDGMENTS

The authors wish to thank the STNA for supporting this research, and SEXTANT for having provided technical assistance.

REFERENCES

Braasch M. (1994) *« Isolation of GPS Multipath and Receiver Tracking Errors »*, in proceedings of ION National Technical Meeting, San Diego, January 24-26.

Braasch M. (1996) *« Global Positioning System: Theory and Applications »*, volume 1, chapter 'Multipath Effects', pages 547-568, AIAA.

Macabiau C., Roturier B., Benhallam A. and Renard A. (1998) *"Development of an end-to-end GPS simulator as a tool for siting GPS reference stations on airport platforms"*, proceedings of ION GPS 98, Nashville, September 15-18.

Macabiau C., Roturier B., Chatre E. and Renard A. (1999) *"Airport multipath simulation for siting DGPS reference stations"*, proceedings of ION National Technical Meeting, San Diego, January 25-27.